JOURNAL OF GEOPHYSICAL RESEARCH, VOL. 105, NO. B8, PAGES 18,965–18,976, AUGUST 10, 2000

Measured and calculated seismic velocities and densities for granulites from xenolith occurrences and adjacent exposed lower crustal sections: A comparative study from the North China craton

Shan Gao,[1, 2, 3] Hartmut Kern,[4] Yong-Sheng Liu,[2] Shu-Yan Jin,[2] Till Popp,[4] Zhen-Min Jin,[2] Jia-Lin Feng,[5] Min Sun,[6] and Zu-Bin Zhao[2]

Abstract. Granulites from the Neogene xenolith-bearing Hannuoba alkaline basalt and from the Manjinggou-Wayaokou exposed lower crustal section in the Archean Huai'an terrain, which occurs within and surrounds the Hannuoba basalt, provide a unique opportunity for a comparative study on petrophysical properties and composition of the lower crust represented by these two types of samples. *P* and *S* wave velocities and densities of 12 Hannuoba lower crustal xenoliths and one associated spinel lherzolite xenolith as well as nine granulites and granulite-facies metasedimentary rocks from the Archean Huai'an terrain were measured in laboratory at pressures up to 600 MPa and temperatures up to 600°C. Calculations of *P* and *S* wave velocities were also made for the same suite of samples based on modal mineralogy and single-crystal velocities whose variations with composition are considered by using microprobe analyses and velocities of end members. The measured and calculated V_p at room temperature and 600 MPa, where the microcrack effect is considered to be almost eliminated, agree within 4% for rocks from the Manjinggou-Wayaokou section and the adjacent Wutai-Jining upper crustal to upper lower crustal section. In contrast, the xenoliths show systematically lower measured V_p by up to 15% relative to calculated velocities, even if decompression-induced products of kelyphite and glass are taken into account. The lower measured velocities for xenoliths are attributed to grain boundary alteration and residual porosity. This implies that although granulite xenoliths provide direct information about lower crustal constitution and chemical composition, they are not faithful samples for studying in situ seismic properties of the lower crust in terms of measured velocities due to alterations during their entrainment to the surface, which changes their physical properties significantly. In this respect, granulites from high-grade terrains are better samples because they are not subjected to significant changes during their slow transport to the surface and because physical properties depend primarily on mineralogy in addition to pressure and temperature. On the other hand, calculated velocities for granulite xenoliths are consistent with velocities for granulites from terrains, suggesting that they can be also used to infer lower crust composition by correlating with results from seismic refraction studies.

1. Introduction

Seismic refraction profiles are one of the most important ways of probing the generally inaccessible deep crust over large areas. Refraction studies give *P* and *S* wave velocities which are determined by the rock composition in addition to pressure, temperature, and fluid [*Kern and Schenk*, 1985, 1988; *Christensen*, 1989; *Fountain and Christensen*, 1989; *Holbrook et al.*, 1992; *Kern*, 1993; *Kern et al.*, 1993, 1996a, b, 1999; *Miller and Christensen*, 1994; *Popp and Kern*, 1994; *Christensen and Mooney*, 1995; *Rudnick and Fountain*, 1995]. The nonuniqueness in relating seismic velocity and rock lithology is one of the major problems in the interpretation of geophysical data, which can be reduced by measurement of seismic properties of regional deep crustal rocks at in situ conditions and with combined use of compressional and shear wave velocities and heat flow data [*Holbrook et al.*, 1992; *Rudnick and Fountain*, 1995; *Kern et al.*, 1996a, b].

Granulite xenoliths brought to the surface mainly by basaltic volcanics and exposed granulite terrains provide direct windows into the present and/or fossil lower crust. However, they are rare in occurrence. Although seismic velocities and densities of lower crustal rocks from type exposed lower crustal cross sections like the Ivrea zone [*Fountain*, 1976; *Barruol and Kern*, 1996], the Calabria zone [*Kern and Schenk*, 1985, 1988], the Kapuskasing Structure Uplift [*Fountain et al.*, 1990; *Salisbury and Fountain*, 1994], the Kohistan accreted terrane [*Miller and Christensen*, 1994], and the Wutai-Jining zone, the North China craton [*Kern et al.*, 1996b] have been measured, few lower crustal xenoliths [*Jackson and Arculus*, 1984; *Jackson et al.*, 1990; *Rudnick and*

[1]Department of Geology, Northwest University, Xi'an, China.
[2]Faculty of Earth Sciences, China University of Geosciences, Wuhan, China.
[3]Department of Earth and Planetary Sciences, Harvard University, Cambridge, Massachusetts.
[4]Institut für Geowissenschaften, Universität Kiel, Kiel, Germany.
[5]Department of Geology, Shijiazhuang College of Economics, Shijiazhuang, China.
[6]Department of Earth Sciences, The University of Hong Kong, Hong Kong.

Paper number 2000JB900100.
0148-0227/00/2000JB900100$09.00

Jackson, 1995] have been studied for seismic velocity due to their sizes which are usually too small for measurement.

Major differences exist between lower crustal rocks of different types. Granulite xenoliths are mostly found in Mesozoic-Cenozoic basalt and are dominated by mafic compositions, whereas granulite terrains are dominantly Archean and have more silicic compositions [*Griffin and O'Reilly*, 1987; *Bohlen and Mezger*, 1989; *Fountain et al.*, 1990; *Rudnick and Presper*, 1990; *Rudnick*, 1992; *Rudnick and Fountain*, 1995]. On the basis of equilibration pressure, *Bohlen and Mezger* [1989] suggested that these two types of granulites are samples of different levels of the crust: isobarically cooled granulite terrains equilibrated at middle to lower crustal levels (600 to 800 MPa), whereas xenoliths represent the underplated lowermost crust (1000 to 1500 MPa). However, *Rudnick and Fountain* [1995] show that it is not possible, on the basis of geobarometry, to distinguish differences in derivation depths between terrains and xenoliths. Therefore genesis of differences between these two types of lower crustal samples is still a matter of great controversy, which is critical for evaluation of formation, evolution, and composition of the lower continental crust. One of the important approaches to unraveling the problems is to make comparative petrological, geochemical, and petrophysical study of these two types of granulites that occur adjacently in the area where seismic refraction/reflection data are available. Granulite terrains are mainly Archean, whereas very few granulite xenolith localities are situated in Archean crust [*Rudnick*, 1992], and opportunities are rare [*Roberts and Ruiz*, 1989]. The northern margin of the North China craton provides one of such opportunities where the granulite- and peridotite xenoliths-bearing Neogene Hannuoba alkaline basalt is underlain and surrounded by Archean granulite terrains. The area is peculiar in several aspects. First, the basalt erupted through the Archean Huai'an granulite terrain, which is exposed at the surface and is proposed to represent an exposed lower crustal section along the Manjinggou-Wayaokou zone [*Zhai*, 1996]. Exposed lower crustal sections like the Ivrea zone and Kapuskasing Structure Uplift are generally considered to reside in the present regional deep crust [*Fountain*, 1976; *Fountain et al.*, 1990; *Salisbury and Fountain*, 1994; *Barruol and Kern*, 1996]. Therefore both the Hannuoba granulite xenoliths and granulites from the Huai'an terrains should exist in the present deep crust of the North China craton, which makes it possible to directly correlate data from seismic profiles with in situ measurements of seismic velocities of xenoliths and terrain rocks. Second, the granulite xenoliths are unweathered, have a diverse variety of composition and quite unusually large size of 10-60 cm in diameter, and may have sampled varying depths of the lower crust, all of which make

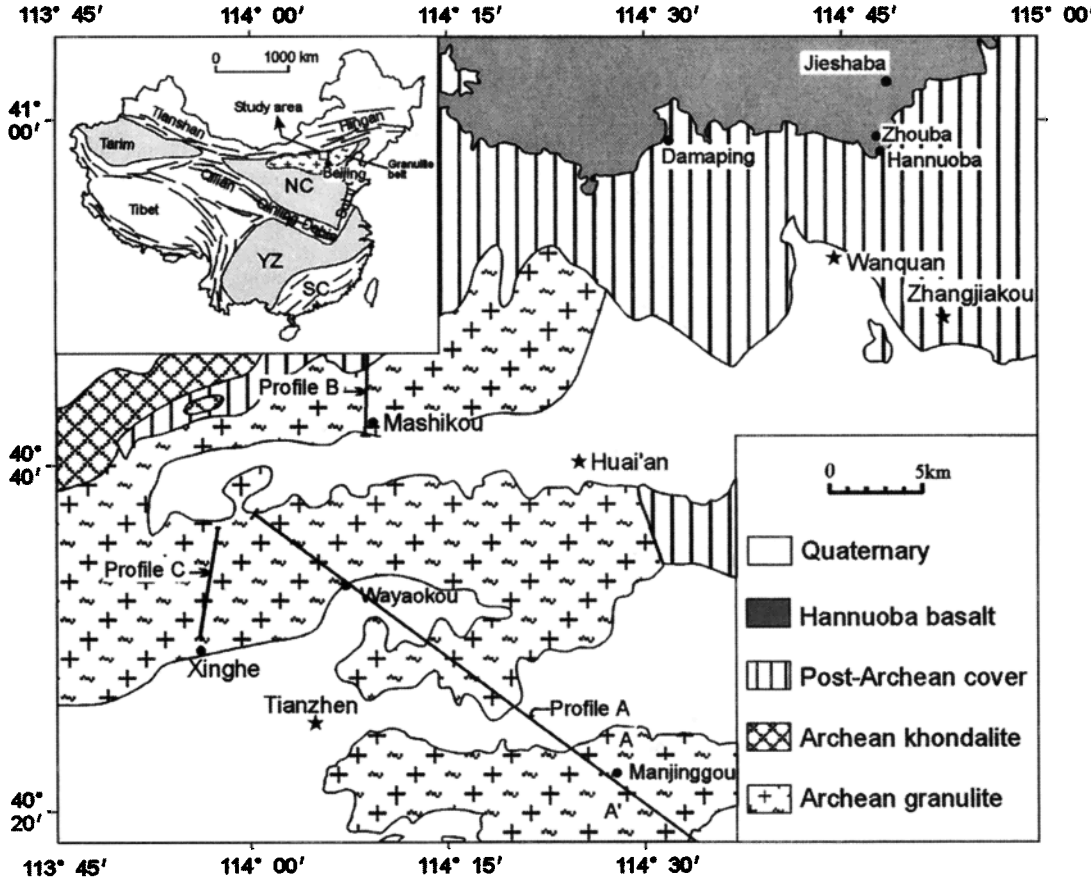

Figure 1. Simplified geological map of the Hannuoba-Huai'an area. Profiles A and B indicate the sections from Manjinggou to Wayaokou and from Mashikou northward to Shangyi (not shown) of the Huai'an terrain, and profile C denotes the Xinghe section of the Jining terrain. Profiles A and B and profile C are proposed to represent two exposed lower crust sections [*Kern et al.*, 1996b; *Zhai*, 1996]. Samples used in this study for the Huai'an terrain are taken from profile A. Inset shows location of the study area, distribution of the granulite belt along the northern margin of the North China craton, and tectonic division of China, where dashed lines denote orogenic belts. NC, North China craton; YC, Yangtze craton; SC, South China orogen.

them rare for petrophysical and geochemical studies. Third, garnet-bearing mafic granulites from the Huai'an terrain were equilibrated at pressures 0.9-1.4 Ga [*Zhai*, 1996], which is comparable to or even higher than pressures recorded by the granulite xenoliths. Fourth, seismic refraction/reflection profilings were conducted extensively in this and the adjacent parts of the North China craton [*Gao et al.*, 1998] because of earthquake activities in the area. Finally, the North China craton generally shows a sharp velocity contrast between the lower crust and upper mantle [*Gao et al.*, 1998]. For example, in the Hannuoba area the *P* wave velocities increase from 7.0 to 8.0 km s^{-1} from the base of the crust to the upper mantle [*Zhu et al.*, 1997]. This implies that the present-day crust-mantle boundary is not transitional with the coincidence of the petrological and geophysical Moho, which is supported by studies of xenoliths from Hannuoba [*Chen*, 1996] and Nushan [*Xu et al.*, 1998].

This paper presents *P* and *S* wave velocities and densities measured in the laboratory at pressures up to 600 MPa and temperatures up to 600°C for 12 Hannuoba lower crustal xenoliths and one associated spinel lherzolite xenolith as well as nine granulites and granulite-facies metasedimentary rocks from the Archean Huai'an terrain. The data are used to answer which of these two types of granulites is representative of the lower crust petrophysically.

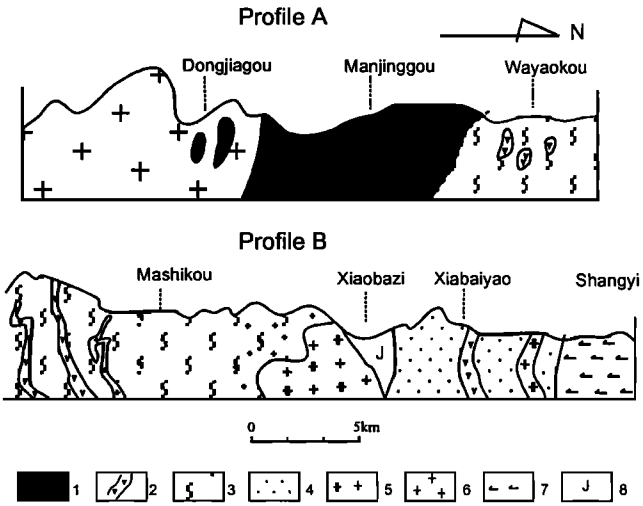

Figure 2. Geological cross sections from Manjinggou to Wayaokou (profile A) and from Mashikou northward to Shangyi (profile B)[after *Zhai*, 1996]. See Figure 1 for location of the profiles. 1, high-pressure granulite with a dominant mafic composition; 2, mafic granulite enclaves; 3, intermediate granulite; 4, garnet- and sillimanite-bearing metasedimentary rock; 5, charnockite; 6, granite; 7, amphibolite-facies rocks; 8, Jurassic sediments.

2. Geological Setting

The North China craton (Figure 1) is one of the world's oldest Archean cratons and preserves crustal remnants as old as 3.8 Ga [*Liu et al.*, 1992]. It experienced widespread tectonothermal reactivation during Late Mesozoic and Cenozoic, as indicated by emplacement of voluminous Late Mesozoic granites and extensive Cenozoic volcanism. The tectonothermal events resulted in replacement of the old, cold, thick, and depleted lithospheric mantle by young, hot, thin, and fertile lithospheric mantle accompanied by lithospheric thinning [*Griffin et al.*, 1998]. A huge Archean granulite belt extending E-W for over 1000 km is distributed in the central part of the northern North China craton (Figure 1). The Huai'an terrain is located in the central part of the belt (Figure 1) and consists of two-pyroxene-bearing tonalitic gneiss, garnet-bearing two-pyroxene granulite, and two-pyroxene granulite as well as metapelite, metasandstone, and marble. All these rocks were subjected to granulite-facies metamorphism. Detailed geological studies suggest that the rock sequence in Manjinggou-Wayaokou (profile A) and from Mashikou northward to Shangyi (not shown) (profile B, Figure 1) represents an exposed lower crust section [*Zhai*, 1996]. The section shows a systematic northward decrease in metamorphic grade from high-granulite to epidote-amphibolite facies from Manjinggou to Shangyi (Figure 2) with a metamorphic pressure decrease from 1.4 GPa to 0.5 GPa [*Zhai*, 1996]. This is accompanied by increasing proportions of intermediate and felsic rocks upward in the section. The high granulite-facies rocks in Manjinggou are dominated by garnet-bearing mafic granulite, while tonalitic granulite and charnockite are the major rock types in Wayaokou and Mashikou and garnet- and sillimanite-bearing metapelite and metasandstone dominate north of the Mashikou. The lower part of the section in Manjinggou is in fault contact with granite to the south, suggesting the lowermost crust being unexposed in the section.

Adjacent to the Manjinggou-Wayaokou section, the Wutai-Jining zone is proposed to represent an upper crustal to upper lower crustal section with the 5-km-thick lowermost crust (V_p>7.0 km s^{-1}) being unexposed based on geological and petrophysical evidence and by correlating measured seismic velocities of rocks with results from seismic refraction profiles [*Kern et al.*, 1996b]. The Xinghe section (profile C, Figure 1) constitutes the lower crust part of the Wutai-Jining zone. The Huai'an and Jining terrains are considered to belong to the same terrain because of their proximity in space and similar rock associations. Geothermobarometric studies using the two-pyroxene and garnet assemblage indicate metamorphic pressures of 1.0-1.4 and 0.7-1.0 GPa for the Huai'an and Jining terrains, respectively [*Kern et al.*, 1996b; *Zhai*, 1996]. Mafic granulite and associated tonalitic-trondhjemitic gneisses from Manjinggou-Wayaokou have a whole rock Sm-Nd isochron age of 2705 ± 40 Ma [*Liu*, 1999].

The Hannuoba alkaline basalt occurs immediately north of Huai'an-Wanquan-Zhangjiakou (Figure 1) and extends north to the Inner Mongolian Province, covering an area of >1700 km^2. The volcanism was related to the widespread Cenozoic rifting in the North China craton. Lower crustal and upper mantle xenoliths carried by the basalt show a diverse variety of rock types. The lower crustal xenoliths include mafic, intermediate, and felsic granulites with the mafic types dominant. The mantle wall rock peridotite xenoliths are dominated by spinel lherzolite with minor webserite and rare garnet-bearing spinel lherzolite [*Feng et al.*, 1982; *Chen*, 1996]. In addition to granulites and peridotites, pyroxenites are also abundant. Each of the mafic and felsic granulites and pyroxenites contains a garnet-bearing variety, and garnet is, in general, partly to totally replaced by dark kelyphite consisting of extremely fine-grained plagioclase, pyroxene, and spinel. The granulite xenoliths occur mostly at Damaping (Figure 1) and are dominantly mafic with less important intermediate and felsic members. They were formed by fractional crystallization of pyroxene and plagioclase from underplated and overplated basaltic magma chamber near the crust-mantle boundary [*Liu*, 1999]. In contrast, granulite xenoliths from Zhouba are

exclusively intermediate and felsic, and some contain graphite and sillimanite, indicating a sedimentary protolith. Xenoliths from Jieshaba are small in size (<2 cm in diameter) and consist of mafic to felsic granulites with rare garnet two pyroxenite exhibiting typical granular texture.

Chen [1996] and *Chen et al.* [1996] made a detailed study of P-T conditions for the Hannuoba lower crustal and upper mantle xenoliths using microprobe analysis of minerals after careful selection of suitable geothermobarometers according to *Xu et al.* [1998]. For temperature estimation the two-pyroxene geothermometer of *Wells* [1977] was applied to two-pyroxene granulite; the geothermometer of *Brey and Kohler* [1990] based on the Ca content of orthopyroxene was applied to pyroxenite; the two-pyroxene geothermometer of *Brey and Kohler* [1990] was applied to Mg-rich (Mg # > 0.80) (Mg # = 100×Mg/(Fe + Mg)) garnet-bearing pyroxenite; the garnet-clinopyroxene geothermometer of *Elllis and Green* [1979] was applied to Fe-rich (Mg#<0.80) garnet-bearing pyroxenite; and the orthopyroxene-spinel geothermometer of *Sachtleben* and *Seck* [1981] was applied to spinel lherzolite and garnet-bearing spinel lherzolite. Pressure was estimated only for garnet-bearing pyroxenite using the garnet-pyroxene geothermometers of *Brey and Kohler* [1990] and *Wood* [1974] for the Mg-rich and Fe-rich garnet-bearing members, respectively. The results show that although there are overlaps in the P-T conditions, different types of xenoliths have distinct ranges. Temperatures of all the 22 analyzed mafic granulites are below 950°C and dominated by 850-950°C. The estimated temperatures are independent of the composition of pyroxene, suggesting equilibrium between orthopyroxene and clinopyroxene. The spinel lherzolite ranges from 850 to 1050°C, and garnet-bearing spinel lherzolite ranges from 1050 to 1100°C. The pyroxenite falls in the range of 800-1000°C with 950-1000°C dominant, while garnet-bearing pyroxenite formed at 1040-1170°C and 1700-1900 MPa and thus represents deepest samples of the Hannuoba xenolith populations. Using the same geotherometers, *Liu* [1999] also estimated equilibrium temperature of mafic granulites to range from 890 to 910°C, which is similar to the above results.

Two pyroxenes are absent from the intermediate and felsic granulites at Zhouba. However, estimates based on the two-feldspar geothermometer of *Powell and Powell* [1977] yield temperature between 718 and 786°C [*Liu*, 1999].

The paucity of pressure estimates prevents construction of a geotherm from the Hannuoba xenoliths. However, the P-T conditions for the Hannuoba garnet-bearing pyroxenites fall on the geotherm [*Xu et al.*, 1998] from lower crustal and upper mantle xenoliths at Nushan along the southern margin of the North China craton [*Chen*, 1996]. By referring to the Nushan geotherm the temperature estimates for the Hannuoba xenoliths suggest that the intermediate and felsic granulites were derived from the depth of 20-25 km, mafic granulites from the depth of 30-40 km, pyroxenite and spinel lherzolite from the depth of 40-55 km, and garnet-bearing spinel lherzolite and garnet-bearing pyroxenite from the depth of 55-70 km. The Moho is at 40-42 km [*Zhu et al.*, 1997]. The overlap in the lower-temperature side (800-950°C) of the pyroxenite and spinel lherzolite with the mafic granulite implies that these two rock types might also exist at the base of the crust in addition to the mafic granulite. However, their considerably higher than the lowermost crust velocities (V_p=7.3-8.2 km s^{-1}) infer that these two rock types cannot be abundant in the lower crust.

The Hannuoba basalt is dated to be 14-27 Ma by the K-Ar method [*Zhu*, 1998]. U-Pb dating of single zircons separated from one Damaping mafic granulite xenolith yields a concordant age range of 121-140 Ma, which is interpreted to represent the timing of basaltic underplating leading to granulite-facies metamorphism [*Fan et al.*, 1998]. Although the Nd isotopic composition is largely homogenized at the mineral scale, whole rock samples of the Damaping granulites also give an imprecise Sm-Nd isochron age of 145 Ma (Y.-S. Liu et al., Geochronology of lower crustal xenoliths: Implications for a dynamic continental crust at the northern margin of the North China craton, submitted to Chemical Geology, hereinafter referred to as Liu et al., submitted manuscript, 2000). Whole rock and garnet and plagioclase separates from one Zhouba granulite (ZB-22) of a clastic sedimentary protolith yield a Sm-Nd isochron age of 424 ± 10 Ma, which is interpreted to represent the age of another phase of granulite-facies metamorphism unrelated to the Mesozoic event (Liu et al., submitted manuscript, 2000). Detrital zircon dating by the evaporation method for the same sample produces an age range from 727 to 1551 Ma, which is considered to represent the age of the source provenance (Liu et al., submitted manuscript, 2000).

Microstructurally, the granulite xenoliths are different from granulites from the Huai'an and Jining terrains in several aspects: (1) marked microfracturing due to rapid decompression during uplift, (2) disaggregation of grain boundaries, (3) melt infiltration as documented by quenched glass, (4) mineral reactions on grain boundaries, and (5) retrogressive alteration (e.g., replacement of garnet by kelyphite and alteration of plagioclase via zeolite).

3. Samples and Experimental Technique

Seismic velocities and densities were measured for 12 granulite and pyroxenite xenoliths and one peridotite xenolith from Damaping and nine granulites from the Manjinggou-Wayaokou section. Because the Zhouba and Jieshaba xenoliths are either fragmented or small in size, they are not measured for petrophysical properties.

Cube-shaped specimens with a 43-mm edge length were used for velocity measurement. Compressional (V_p) and shear (V_s) wave velocities were measured on oven-dry rocks using the ultrasonic pulse transmission technique. The sample reference system corresponds to fabric elements (normal to foliation [*Z*], perpendicular to lineation [*Y*], and parallel to lineation [*X*]). The special arrangement of the apparatus allows simultaneous measurements of *P* and *S* wave velocities along the three directions *X*, *Y*, and *Z* of the sample cubes.

A state of near hydrostatic stress is obtained by advancing six pyramidal pistons in three mutually orthogonal directions onto specimens [*Kern et al.*, 1997]. A furnace surrounds one end of each piston next to the specimen, and heat is transmitted from the pistons to the specimen. Thus a very homogeneous heating and distribution of temperature is achieved within the large-volume specimens, which has been confirmed by temperature measurements at different places within a test sample. Temperature is measured using thermocouples placed in a cavity at the end of each piston very close (~1 mm) to the specimen. Compressional and shear waves were generated by means of 2 and 1 MHz, respectively, lead titanate zirconate (PTZ) transducers. The transducers are placed on the low-temperature side of the pistons. The travel time of the pulses through the specimen is obtained by subtracting the calibrated time needed for the pulse to travel to and from the specimen through the pistons from the total time measured by the transducers. The *P* and *S* wave velocities were measured simultaneously in the three

Table 1. Modal Composition of Minerals Based on Point Counting for Hannuoba Xenoliths and Rocks From Huai'an Terrain

Rock Type	Sample	Pl	Ksp	Qz	Cpx	Opx	Kely	Gt	Ap	Op	Glass	Ol	Sp	Bi	Amp	Rutile
							Hannuoba xenolith									
Spinel lherzolite	DMP-04				4.6	34.9						60.2	0.3			
Garnet-bearing	DMP-07	65.86			5.78	2.26	5.70			0.73	19.68					
mafic granulite	DMP-08	13.15			35.60	9.78	41.48									
Mafic granulite	DMP-06	63.80			15.43	4.84			0.25	3.92	11.76					
	DMP-09	29.91			42.72	27.37										
	DMP-66	43.55			49.24	7.20										
	DMP-71	21.75			71.63	6.61										
Plagioclase-bearing	DMP-49	2.80			85.51	5.04					6.65					
pyroxenite	DMP-68	3.74			81.20	14.81				0.26						
Pyroxenite	DMP-10				73.13	26.87										
	DMP-11				69.58	29.34				1.08						
	DMP-14				17.88	9.83						72.30				
Intermediate granulite	DMP-70	50.46	4.69		6.32	2.77			0.33	0.35	35.08					
							Huai'an terrain									
Garnet-bearing mafic granulite	MQG-15	26.97	1.02		3.14	15.76		12.59							40.52	
Mafic granulite	MQG-02	43.50	3.29		18.09	24.79				2.10					8.23	
	WYK-09	56.08	0.64		24.31	14.37				4.61						
Intermediate	MQG-01	78.23		4.38	2.18	13.65				1.27				0.28		
granulite	MQG-20	58.00			18.94	9.36				7.85				0.36	5.49	
Felsic granulite	WYK-06	67.99	0.10	21.21	4.94	3.03			0.68	2.05						
Garnet-bearing metasandstone	MQG-05	17.30		35.00	4.51	15.39		25.37						0.60	0.78	1.05
Garnet-bearing metapelite	MQG-06	40.33		8.17	8.61	19.06		20.58		2.82				0.43		
Metapelite	MQG-08	36.34	1.95		22.68	17.57								21.47		

Pl, plagioclase; Ksp, K-feldspar; Qz, quartz; Cpx, clinopyroxene; Opx, orthopyroxene; Kely, kelyphite; Gt, garnet; Ap, apatite; Op, opaque mineral; Ol, olivine; Sp, spinel; Bi, biotite; Amp, amphibole.

orthogonal directions. Splitting of shear waves is obtained for each direction of propagation by two sets of transducers with perpendicular planes. Length and resulting volume changes of the sample cubes due to changes of principal stress and temperature are obtained from the piston displacement. Densities for each sample (oven-dried) were calculated from the masses and the measured volumes of the cubes. Each set of results is composed of three P wave velocities and six S wave velocities and pressure- and temperature-dependent volumetric strain.

Measurements were done at pressures up to 600 MPa at room temperature and from room temperature up to 600°C at 600 MPa confining pressure. Wave velocities were measured at ~50-MPa intervals during pressure increase to 600 MPa. Maintaining the hydrostatic pressure of 600 MPa constant overnight, the temperature was increased the following day in steps of ~80°C over ~15-min periods. To ensure that the samples had reached pressure and temperature equilibrium, successive readings were taken at time intervals of at least 30 min. The cumulative error in V_p and V_s is estimated to be <1%.

4. Results and Discussion

4.1. General Characteristics

Tables 1 and 2 give modal mineral compositions based on point counting and major element composition for the measured Damaping xenoliths and granulites and granulite-facies metasedimentary rocks from the Manjinggou-Wayaokou section. Neglecting clastic metasedimentary rocks from the Manjinggou-Wayaokou section and the spinel lherzolite xenolith, the weight percent SiO_2 of the measured rocks falls in the range 45.3-64.2%, pointing to felsic (>63% SiO_2), intermediate (63-52% SiO_2), and mafic (45-52% SiO_2) compositions according to the scheme for

Table 2. Major Element Composition of Hannuoba Xenoliths and Rocks from Huai'an Terrain

Rock Type	Sample	SiO_2	TiO_2	Al_2O_3	Fe_2O_3	FeO	MnO	MgO	CaO	Na_2O	K_2O	P_2O_5	H_2O^+	CO_2	Total	Mg #
							Hannuoba xenolith									
Spinel lherzolite	DMP-04	43.76	0.06	2.14	0.79	6.97	0.12	42.97	2.01	0.12	0.10	0.02	0.81	0.04	99.91	90 89
Garnet-bearing	DMP-07	45.71	0.62	24.44	2.54	3.55	0.06	5.07	12.09	2.31	0.33	0.05	2.80	0.13	99.70	60 77
mafic granulite	DMP-08	45.27	0.55	17.16	1.99	7.08	0.12	12.42	12.06	1.36	0.10	0.04	1.55	0.04	99.74	71 40
Mafic granulite	DMP-06	51.72	0.96	18.06	2.05	5.10	0.12	6.97	5.41	4.03	1.78	0.27	3.10	0.04	99.61	64.15
	DMP-09	49.54	0.49	9.65	1.17	8.33	0.15	18.37	8.17	1.23	0.35	0.02	2.11	0.03	99.61	77.73
	DMP-66	50.51	0.42	12.10	0.94	6.17	0.12	13.58	12.14	1.62	0.33	0.02	1.71	0.03	99.69	77.53
	DMP-71	49.60	0.60	9.61	1.58	8.57	0.17	13.98	12.12	1.21	0.47	0.05	1.63	0.09	99.68	71.38
Plagioclase-bearing	DMP-49	50.16	0.57	7.64	1.86	7.68	0.17	16.44	12.77	0.79	0.30	0.02	1.25	0.04	99.69	75.81
pyroxenite	DMP-68	49.74	0.41	9.41	0.74	7.75	0.15	16.23	11.30	1.91	0.17	0.03	1.81	0.07	99.72	77 47
Pyroxenite	DMP-10	48.99	0.69	5.81	2.39	8.37	0.18	18.62	12.82	0.42	0.10	0.02	1.31	0.04	99.76	75.93
	DMP-11	49.83	0.52	4.68	1.18	9.77	0.18	20.18	11.45	0.40	0.10	0.02	1.01	0.48	99.80	76.86
	DMP-14	50.89	0.24	5.75	1.11	4.10	0.13	20.51	15.32	0.53	0.10	0.02	0.74	0.22	99.66	87.76
Intermediate granulite	DMP-70	56.82	0.55	15.20	1.71	3.55	0.09	5.34	5.10	2.93	4.52	0.25	3.45	0.04	99.55	65.17
							Huai'an terrain									
Garnet-bearing mafic granulite	MQG-15	45.80	1.43	14.28	2.68	11.97	0.22	8.61	12.20	1 53	0.16	0.13	0.59	0.18	99.78	51.63
Mafic granulite	MQG-02	45.55	0.99	13.78	3.49	11.58	0.26	9.36	12.21	1.27	0.28	0.04	0.81	0.18	99 80	53.13
	WYK-09	50.54	1.43	12.94	4.44	10.37	0.22	6.07	10.11	2.45	0.21	0.12	0.70	0.09	99.69	42.96
Intermediate	MQG-01	57.86	0.71	16.74	1.30	7.05	0.12	3.52	6.55	4.17	0.74	0.17	0.68	0.04	99.65	43.29
granulite	MQG-20	54.30	1.46	13.68	5.04	9.38	0.27	4.38	6.93	2.80	0.88	0.27	0.29	0.11	99.79	35.94
Felsic granulite	WYK-06	64.21	0.58	16.81	1.30	3.05	0.05	1.84	5.01	4.82	1.10	0.24	0.57	0.09	99 67	43.74
Garnet-bearing metasandstone	MQG-05	59.65	0.82	20.85	0.34	8.07	0.05	2.90	1.07	0.96	3.79	0.08	0.96	0.09	99.63	38.16
Garnet-bearing metapelite	MQG-06	44.72	2.40	12.75	0.50	19.48	0.35	7.10	9.53	0.61	0.62	0.24	1.07	0.44	99.81	38.84
Metapelite	MQG-08	55.79	0.96	13.91	1.48	7.18	0.11	5.96	5.90	1.86	2.27	0.09	1 34	2.73	99.58	55 52

Mg #, magnesium number, 100×Mg/(Fe+Mg) (in atomic number).

igneous rocks proposed by the International Union of Geological Sciences [*Le Bas and Streckeisen*, 1991].

The mafic-ultramafic rocks include garnet-bearing mafic granulite, mafic granulite, plagioclase-bearing pyroxenite, and pyroxenite. Major element compositions vary clearly with the subdivisions of mafic rocks. For example, compared to the counterparts without garnet, the garnet-bearing mafic granulite xenoliths contain significantly lower SiO_2, which is coupled by remarkably higher Al_2O_3 (Table 2). The plagioclase-bearing pyroxenites are characterized by being high in Al_2O_3 and Na_2O and low in MgO compared to the pyroxenites.

Table 3 summarizes data on measured bulk densities, average P and S wave velocities as well as pressure and temperature derivatives of wave velocities. As an example, a complete set of the nine velocities for mafic granulite xenolith DMP-09 is plotted in Figure 3 for the pressure range 20-600 MPa. Also shown are the P wave velocities for the temperature range 20-600°C measured at 600 MPa confining pressure. At increasing confining pressure, P and S wave velocities typically show a nonlinear velocity increase up to ~200 MPa (Figure 3), which is interpreted in terms of closure of the microcracks. At higher pressures a slight, linear increase of velocities is observed. Increase of temperature at high confining pressure (600 MPa) results in a slight, linear decrease in the wave velocities. Like rocks from other metamorphic terrains [*Kern and Schenk*, 1988; *Kern et al.*, 1993, 1996b, 1999; *Barruol and Kern*, 1996], granulites from the Manjinggou-Wayaokou section show a monotonous, linear increase in velocity with increasing pressure and a linear decrease with increasing temperature (not shown). In contrast, some of the Hannuoba granulite xenoliths (DMP-06, -07, -09, -10, -66 and -71) display a complicated behavior characterized by two or three segments of linear decrease in V_p with increasing temperature, as

Table 3. Measured Bulk Densities, Average P and S Wave Velocities, and Pressure and Temperature Derivatives of Wave Velocities

				Pressure Derivative, 10^{-4} km s^{-1} MPa^{-1}		Temperature Derivative, 10^{-4} km s^{-1} °C^{-1}		600 MPa and Room Temperature Parameters						
Rock Type	Sample	V_{p0}	V_{s0}	dV_p/dP	dV_s/dP	dV_p/dT	dV_s/dT	Density, g cm^{-3}	V_p	V_s	V_p/V_s	Poisson's ratio	V_p^{cal}	V_s^{cal}
						Hannuoba xenolith								
Spinel lherzolite	DMP-04	7.93	4.60	1.66	0.00	-1.94	-1.15	3.298	8.03	4.60	1.75	0.26	8.21	4 81
Garnet-bearing	DMP-07	6 13	3.37	3.75	0.41	0.93	0.44	2.786	6.36	3.40	1.87	0.30	6 54	3.69
mafic granulite	DMP-08	6.96	3.90	2.19	-0.01	-2.01	-1.05	3.119	7.10	3.90	1.82	0.28	7.59	4 30
Mafic granulite	DMP-06	6.03	3.36	0.60	-0.42	-4.73	-4.23	2.742	6.07	3.33	1.82	0.28	6.69	3.75
	DMP-09	7.14	4.17	2.94	0.56	-5.84	-3.12	3.180	7.31	4.20	1.74	0.25	7.30	4.14
	DMP-66	7.03	4.00	2.70	0.43	-3.27	-2.30	3.113	7.19	4.03	1.78	0.27	7.15	4.00
	DMP-71	6.80	3.96	4.64	1.46	-4.96	-3.52	3.172	7.08	4.05	1.75	0.26	7.37	4.16
Plagioclase-	DMP-49	6.90	4.07	6.04	2.31	-1.54	-0.75	3.222	7.27	4.21	1.73	0.25	7.47	4.27
bearing pyroxenite	DMP-68	7.02	4.07	3.97	1.02	-2.64	-1.08	3.058	7.26	4.13	1.76	0.26	7.62	4.35
Pyroxenite	DMP-10	6.99	4.11	6.03	2.13	-1.28	-0.45	3.321	7.35	4.23	1.74	0.25	7.68	4.42
	DMP-11	7.24	4.26	4.48	1.08	-2.19	-0.92	3.349	7.51	4.33	1.74	0.25	7 68	4.43
	DMP-14	7.57	4.46	4.69	1.46	-1.89	-0.76	3.314	7.85	4.55	1.73	0.25	8.33	4 86
Intermediate granulite	DMP-70	5.29	2.91	-0.78	-0.54	1.77	-0.58	2.537	5.24	2.87	1.82	0.29	6.14	3.54
						Huai'an terrain								
Garnet-bearing mafic granulite	MQG-15	7.25	4.14	3.51	0.76	-1.21	-0.19	3.318	7.45	4.18	1.78	0.27	7.19	4.00
Mafic granulite	MQG-02	7.09	4.02	2.51	0.48	-1.46	-0.236	3.214	7.24	4.05	1.79	0.27	7.08	3.97
	WYK-09	6.81	3.87	3.44	-0.39			3.096	6.92	3.86	1.79	0.27	7.06	3.94
Intermediate	MQG-01	6.35	3.67	3.73	0.90	-1.46	-0.11	2.850	6.57	3.72	1.76	0.26	6.53	3.73
granulite	MQG-20	6.59	3.74	3.15	0.55	-1.44	-0.12	3.017	6.77	3.77	1.79	0.27	6.79	3.83
Felsic granulite	WYK-06	6.34	3.68	2.33	0.07	-2.71	-0.70	2.768	6.47	3.68	1.76	0.26	6.38	3.68
Garnet-bearing metasandstone	MQG-05	6.68	3.96	3.65	1.57	-1.72	-0.39	3.035	6.89	4.03	1.71	0.24	6.97	4.16
Garnet-bearing metapelite	MQG-06	7.33	4.13	1.77	-0.01	-2.79	-1.06	3.446	7.43	4.13	1.80	0.28	7.18	4.05
Metapelite	MQG-08	6.39	3.58	3.52	0.85	-2.35	-1.16	2.993	6.60	3.63	1.82	0.28	6.61	3.68

V_p^{cal} and V_s^{cal} are calculated velocities based on modal mineral compositions and velocities of corresponding single minerals given in Table 4 Detailed data on V_p and V_s variations with pressure and temperature are available from G.S. upon request.

exemplified in Figure 3. The inflection commonly occurs at 300°C (DMP-06, -09, -66 and -71; Figure 3). The unusual velocity-temperature relationship with a marked velocity decrease around 300°C must be attributed to dehydration of the zeolite-like minerals. Zeolite is known to contain a great deal of structurally bound water. Part or all of this water is given off continuously or abruptly on heating from room temperature to ~350°C. Dehydration reactions will produce solid-fluid systems, thus leading to a significant decrease of effective pressure, which gives rise to widening of old cracks and to the formation of new cracks. The abrupt increase of pore space and the reconstitution of pore geometry result in a marked decrease of wave velocities [*Kern and Richter*, 1979].

P-wave anisotropy and shear wave splitting are highest (V_p-anisotropy = 6.0-8.1%; V_s//foliation = 0.18-0.38) for spinel lherzolite DMP-04, plagioclase-bearing pyroxenite DMP-68 and

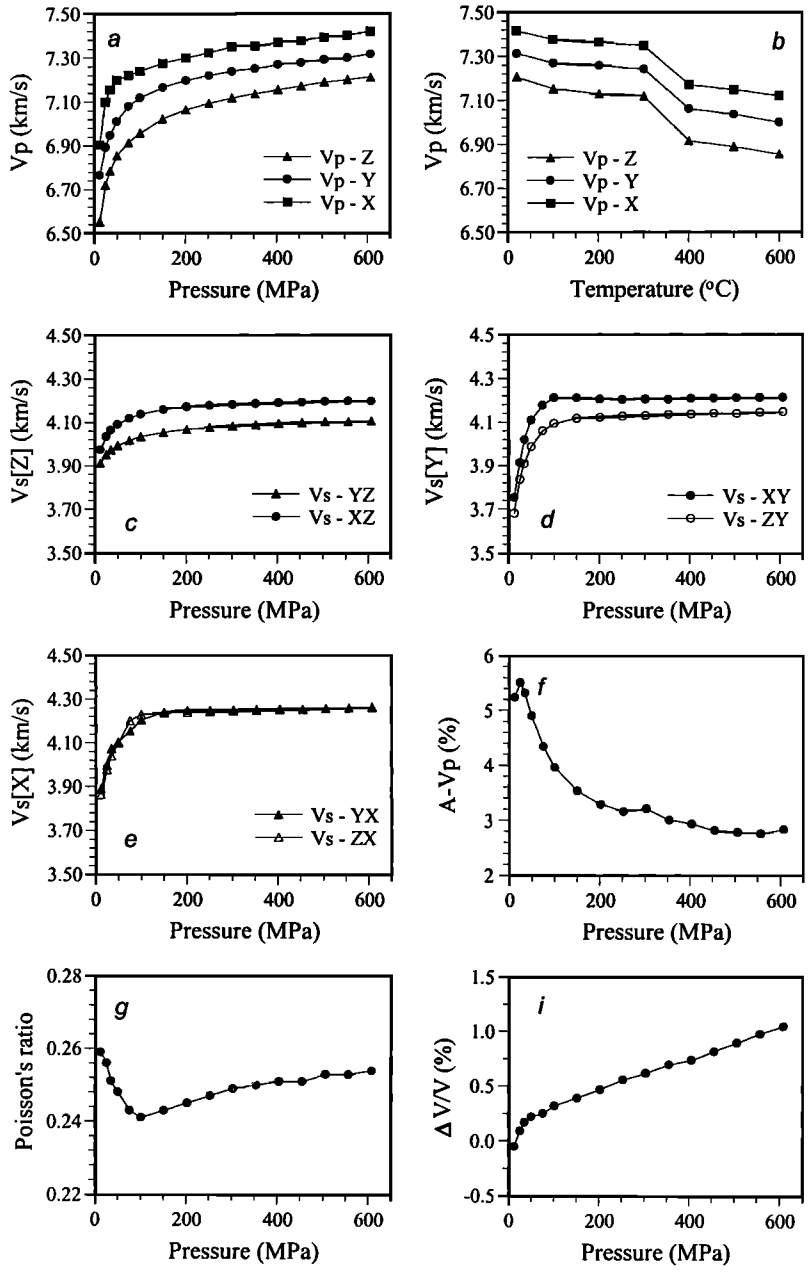

Figure 3. Effect of pressure and temperature on *P* and *S* wave velocities and their directional dependence for the Hannuoba mafic granulite xenolith DMP-09. (a) V_p as a function of pressure at room temperature; (b) V_p as a function of temperature at 600 MPa confining pressure; (c) to (e) shear wave splitting in three structural directions (*X*, *Y*, and *Z*) as a function of pressure.

metapelite MQG-08, which is due to mineral alignment. Other samples have V_p- anisotropy <3.5% and V_s // foliation ≤0.10.

From the regression of the linear segments of the pressure (300-600 MPa) and temperature curves (20-600°C) the pressure and temperature derivatives of velocities and the reference velocities V_{zero} were obtained (Table 3). They allow one to extrapolate seismic velocities for any P-T condition within the stability field of the constituent assemblage of rock-forming minerals.

The pressure derivatives of rocks obtained from this study ($0.6\text{-}6\times10^{-4}$ km s^{-1} MPa) are generally higher than values ($1\text{-}2\times10^{-4}$ km s^{-1} MPa) obtained at pressures above 1000 MPa [e.g., *Christensen*, 1974; *Rudnick and Fountain*, 1995]. This infers that our derived pressure derivatives might not reflect the single-crystal derivatives. As has been shown by *Christensen* [1974], small amounts of the residual low aspect ratio cracks (i.e., spherical pores) are not completely closed at pressures below 1000 MPa. However, the effect of small amounts of spherical pores on wave velocities is generally believed to be low. Most of the high aspect ratio cracks are closed at pressures above ~200-300 MPa, giving rise to a linear behavior of the velocity versus pressure relation (Figure 3). Therefore our data can be considered as to describe the near-intrinsic properties of the aggregates, that is, they describe an upper bound.

Temperature coefficient data for crustal and mantle rocks are scarce in the literature [*Kern*, 1978; *Kern and Richter*, 1981;

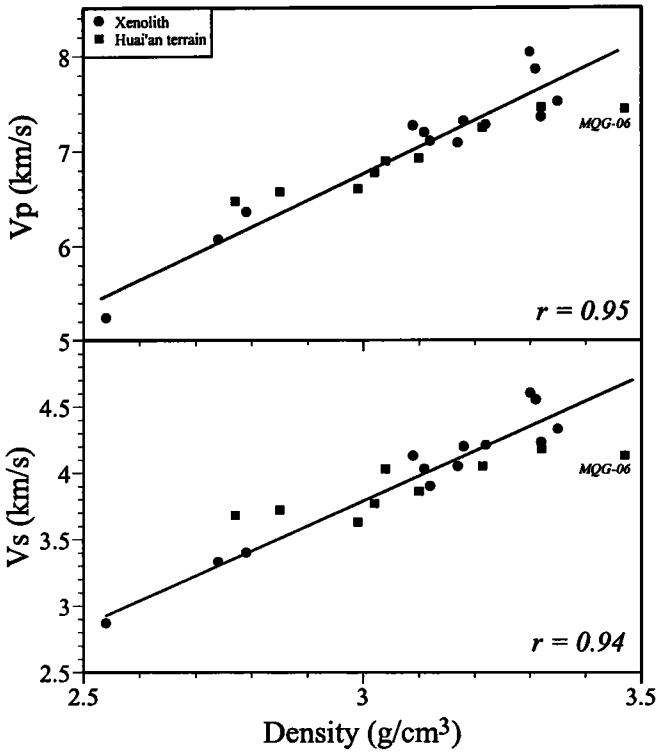

Figure 4. Correlation between density and average seismic velocities at 600 MPa and room temperature for the Hannuoba xenoliths and rocks from the Huai'an terrain. Correlation coefficients (r) exclude sample MQG-06.

Kern and Schenk, 1985, 1988; *Kern et al.*, 1993, 1996a, b, 1999; *Rudnick and Fountain*, 1995]. Studies of *Kern* [1978] and *Kern and Richter* [1981] show that thermally induced microfracturing is increasingly suppressed as pressure is raised and stops at pressures of a few hundred megapascals. The minimum pressure increment needed to prevent thermal cracking has been estimated to be generally around 1 MPa per degree increase in temperature. For the case in which the velocity-temperature relationship is linear at high confining pressure and with a negative slope, the corresponding temperature coefficients of velocities describe the intrinsic behavior fairly well. This is true for terrain rocks and for most of the xenolith samples except DMP-06, -07, -09, -10, -66 and -71. It can be seen from Table 3 that DMP-06, -09, -66 and -71 exhibit considerably higher temperature derivatives than other xenolith samples and terrain rocks.

Figure 4 shows the relationship between velocities and densities measured at 600 MPa. Velocities exhibit a nice positive correlation with density with correlation coefficients being 0.94-0.95.

The plot of silica content against velocities shown in Figure 5 reveals that velocities generally increase with decreasing SiO_2 content. However, the correlation is less significant than the density-velocity correlation. This is because both density and velocity depend primarily on mineralogy, which is a function of metamorphic grade in addition to chemical composition. For example, pyroxenite xenoliths show significantly higher measured and calculated velocities (V_p =7.3-8.3 km s^{-1}) compared to mafic granulites (≤7.4 km s^{-1}) with SiO_2 <52%. (Figure 5 and Table 3). Three granulite xenoliths (DMP-06, -07, and -70) have unusually low measured velocities due to the presence of significant amount of glass and/or kelyphite.

4.2. Comparison of Velocities for Xenoliths and Rocks from Metamorphic Terrains

The fidelity with which the measured velocities reflect the primary mineralogy of rocks can be assessed by comparison of the measured velocities with those calculated for the modal mineralogy from appropriate single-crystal velocity data [*Birch*, 1961; *Jackson et al.*, 1990; *Rudnick and Jackson*, 1995]. To do this, it is important to take into account velocity variations of single minerals with their end-member compositions [*Gebrande*, 1982]. Systemic variations in mineral composition are clear between rock types of the investigation. For example, both clinopyroxene and orthopyroxene from the mafic granulite xenoliths contain significantly less enstatite end-member compared to the pyroxenites and spinel lherzolites [*Chen*, 1996; *Liu*, 1999]. Orthopyroxene in the mafic granulite and pyroxenite xenoliths is enstatite-bronzite and contains 64-76 and 80-90% of the enstatite end-member, respectively. In contrast, orthopyroxene in mafic granulites from the Huai'an terrain is generally hypersthene. Clinopyroxene from the Huai'an terrain also contains higher FeO. We calculate velocities (Table 4) of plagioclase, orthoclase, orthopyroxene, clinopyroxene, garnet, olivine, and spinel for various rock types from microprobe analyses of minerals and velocities of corresponding end members given by *Gebrande* [1982]. Possible velocity variations of glass, biotite, and amphibole are not considered, and the velocity of opaque mineral is taken as that of magnetite. The velocity of kelyphite in Table 4 is assumed to be 10% lower than

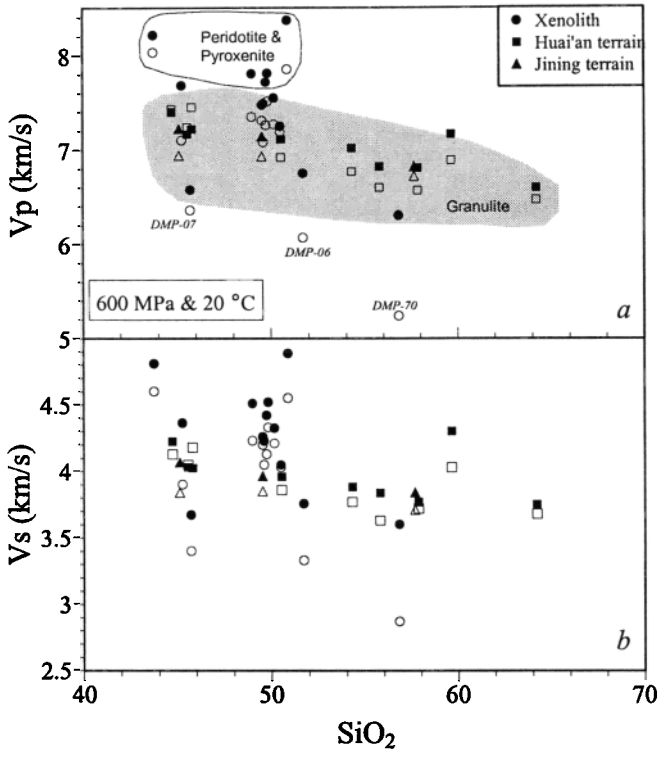

Figure 5. Correlation between SiO_2 content and average (a) compressional and (b) shear wave velocities at 600 MPa and room temperature for the Hannuoba xenoliths and rocks from the Huia'an terrain. Solid and open symbols are for calculated and measured velocities, respectively. Also shown for comparison are data on three granulites from the Jining terrain [*Kern et al.*, 1996b].

Table 4. Single Mineral Elastic Properties Used in Calculation of Rock Velocities

Rock Type	Velocity, km s^{-1}	Pl	Ksp	Qz	Cpx	Opx	Kely	Gt	Ap	Op	Glass	Ol	Sp	Bi	Amp
						Hannuoba xenolith									
Spinel lherzolite	$V_{p\,(VRH)}$				7.66	7.93						8.42	8.36		
	$V_{s\,(VRH)}$				4.35	4.74						4.89	4.56		
Mafic granulite	$V_{p\,(VRH)}$	6.57			7.59	7.63	7.91		6.68	7.39	5.57				
	$V_{s\,(VRH)}$	3.58			4.30	4.49	4.49		3.30	4.20	3.52				
Pyroxenite	$V_{p\,(VRH)}$	6.68			7.62	7.84				7.39	5.57	8.39			
	$V_{s\,(VRH)}$	3.63			4.33	4.66				4.20	3.52	4.85			
Intermediate granulite	$V_{p\,(VRH)}$	6.30	5.60		7.57	7.42			6.68	7.39	5.57				
	$V_{s\,(VRH)}$	3.45	3.05		4.29	4.31			3.30	4.20	3.52				
						Huai'an terrain									
Mafic granulite	$V_{p\,(VRH)}$	6.69	5.63		7.55	7.63		8.94		7.39					6.81
	$V_{s\,(VRH)}$	3.64	3.06		4.28	4.49		5.06		4.20					3.72
Intermediate granulite	$V_{p\,(VRH)}$	6.38		6.05	7.53	7.33				7.39				5.35	6.81
	$V_{s\,(VRH)}$	3.49		4.09	4.26	4.24				4.20				3 00	3 72
Felsic granulite	$V_{p\,(VRH)}$	6.33	5.58	6.05	7.51	7.30			6.68	7.39				5.35	6.81
	$V_{s\,(VRH)}$	3.47	3.03	4.09	4.25	4.21			3.30	4.20				3.00	3.72
Metasandstone	$V_{p\,(VRH)}$	6.38		6.05	7.53	7.26		8.71						5.35	6.81
	$V_{s\,(VRH)}$	3.49		4.09	4.26	4.17		4.89						3.00	3.72
Metapelite	$V_{p\,(VRH)}$	6.50	5.60	6.05	7.54	7.30								5.35	
	$V_{s\,(VRH)}$	3.55	3.05	4.09	4.27	4.21								3.00	

Pl, plagioclase; Ksp, K-feldspar; Qz, quartz; Cpx, clinopyroxene; Opx, orthopyroxene; Kely, kelyphite; Gt, garnet; Ap, apatite; Op, opaque mineral; Ol, olivine; Sp, spinel; Bi, biotite; Amp, amphibole. Velocities of plagioclase, orthoclase, orthopyroxene, clinopyroxene, garnet, olivine and spinel for each rock type are calculated from microprobe analyses of minerals and velocities of corresponding end-members given by *Gebrande* [1982]. Possible velocity variations of glass, biotite, and amphibole are not considered. The velocities of opaque mineral are taken as those of magnetite.

the velocity of garnet. The V_p (7.91 km s^{-1}) thus obtained is substantially the same as that (7.95 km s^{-1}) calculated by *Rudnick and Jackson* [1995] from proportions and single crystal velocities of anorthite, spinel, orthopyroxene, and clinopyroxene, which make up kelyphite. The velocities of the above minerals are then used to calculate the rock velocity (Table 3) according to modal mineral composition based on point counting (Table 1). Figure 6 compares the measured and calculated velocities. Also, Figure 6 shows data for rocks exposed along the Wutai-Jinning zone [*Kern et al.*, 1996b, Figure 1]. It can be seen from Figure 6a that the measured V_p for rocks from the Manjinggou-Wayaokou section and the Wutai-Jining zone is in good agreement with the calculated V_p; the relative difference is within ±4%. In contrast, the xenoliths show systematically lower measured V_p by up to 15% relative to the calculated ones. This is also true for V_s (Figure 6b).

Lower measured relative to calculated *P* wave velocities were also observed from studies of granulite xenoliths from the Chudleigh volcanic province of Australia [*Jackson et al.*, 1990; *Rudnick and Jackson*, 1995] and from upper mantle xenoliths from the Vitim picritic tuff, Russia [*Kern et al.*, 1996a], although generally good agreements between measured and calculated velocities were found for four upper mantle rocks from eastern Australia [*O'Reilly et al.*, 1990]. *Rudnick and Jackson* [1995] summarize five possible causes for lowering measured velocities: (1) scattering of elastic waves at grain boundaries, (2) the presence of significant Al and/or Na in the natural pyroxenes, which are not accounted for in the pyroxene end-members used for the calculations, (3) differences between the modal mineralogy determined on a single thin section and those in the actual rock specimen where the measurements were made, (4) grain boundary alteration in the xenoliths, and/or (5) failure to close all pore spaces due to irreversible changes occurring on grain boundaries or in the process of kelyphitization. They finally ascribe the lower measured velocity to grain boundary alteration and residual porosity. On the basis of the following evidence, it is proposed that their inferences can be also applied to the Hannuoba xenoliths.

1. The velocity discrepancy for xenoliths is unlikely to be due to inaccurate mineral modes because this is difficult to explain the velocity consistency for rocks from the Manjinggou-Wayaokou section and the Wutai-Jinning zone.

2. Velocity variations of minerals with composition have been taken into account.

3. Samples DMP-70 and DMP-06, which show the largest amount of grain boundary alteration characterized by reaction

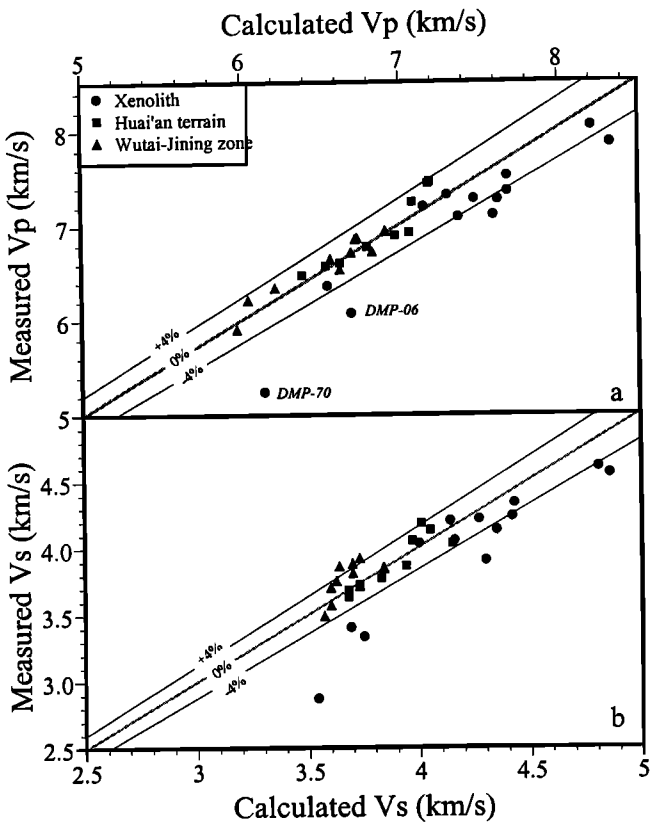

Figure 6. Comparison of calculated and measured (a) compressional and (b) shear wave velocities at 600 MPa and room temperature for the Hannuoba xenoliths and rocks from the Huia'an terrain and from the Wutai-Jining crustal cross section [*Kern et al.*, 1996b]. Equal relative differences between the measured and calculated velocities are shown by lines.

coronas of pyroxene rimmed by amphibole and biotite and by glass and secondary oxides, also show the greatest discrepancy between the measured and calculated velocities.

Another possible explanation for the lower measured velocities is that the applied confining pressure of 600 MPa may not be high enough to completely close all the cracks, as is also suggested by the higher-pressure derivatives. However, the confining pressure is considered unlikely to play a major role in the discrepancy. Otherwise, a positive correlation between dV/dP and the relative calculated versus measured velocity difference would be expected. However, the obtained correlation coefficient for the xenoliths is -0.68 and -0.52 for V_p and V_s, respectively. In addition, as discussed above, the linear behavior of the velocity versus pressure relation at pressures above 200 MPa infers closure of most of the high aspect ratio cracks and only small amounts of the residual low aspect ratio cracks are not completely closed at pressures below 1000 MPa.

It is concluded from the above discussion that although granulite xenoliths are thought to provide direct information about the constitution and chemical composition of the lower crust, they are not faithful samples for studying in situ seismic properties of the lower crust in terms of measured velocities due to occurrence of various alterations during their entrainment to the surface, which change their physical properties significantly. In this respect, granulites from high-grade terrains are better samples because they are not subjected to significant alteration during their slow transport to the surface. This is particularly true because seismic and density properties depend directly on mineralogy and texture of rocks which may or may not correlate with chemical composition. This means that granulite xenoliths should have in situ petrophysical properties similar to the granulites from exposed terrains if they have similar bulk composition, mineralogy, and texture.

On the other hand, it can be seen from Figure 5a that except alteration-affected granulite xenoliths DMP-06, -07 and -70, the other granulite xenoliths and granulites from the Huai'an and Jining terrains form an overall consistent trend on the calculated velocity versus SiO_2 plot. Although significant chemical changes with alteration during xenolith's transport to the surface may occur on the submineral scale, the bulk rock chemical composition is less susceptible to change. This is exemplified by kelyphite, which consists of extremely fine-grained plagioclase, pyroxene, and spinel and which, as whole, generally has the same composition as its precursor of garnet. These results imply that if various alterations are taken into account, calculated velocities of xenoliths could be used to infer the lower crustal composition.

Acknowledgments. This study is cosupported by Chinese Ministry of Science and Technology (grant G1999043202), the Northwest University, the National Nature Science Foundation of China, the Ministry of Education of China, the German Research Society (DFG), and the Hong Kong RGC grant (HKU 7110/97P). We thank N. I. Christensen, I. Jackson and S. Y. O'Reilly for critical comments and P. M. Davis for handling.

References

Barruol, G., and H. Kern, Seismic anisotropy and shear wave splitting in lower-crustal and upper-mantle rocks from the Ivrea-Zone—Experimental and calculated data, *Phy. Earth Planet. Inter.*, *95*, 175-194, 1996.

Birch, F., The velocity of compressional waves in rocks to 10 kilobars, part 2, *J. Geophys. Res.*, *66*, 2199-2224, 1961.

Bohlen, S.R., and K. Mezger, Origin of granulite terranes and the formation of the lowermost continental crust, *Science*, *244*, 326-329, 1989.

Brey, G.P., and T. Kohler, Geothermobarometry in four-phase lherzolite, II, New thermobarometers and practical assessment of existing thermobarometers, *J. Petrol.*, *31*, 1353-1378, 1990.

Chen, S.-H., Structure, composition and interaction of crust and mantle: A petrological study of xenoliths from Hannuoba (in Chinese), Ph.D. thesis, Inst. of Geol., Chin. Acad. of Sci., Beijing, 1996.

Chen, S.-H., M. Sun, X.-H. Zhou, G.-H. Zhang, and J.-L. Feng, Pyroxenitic and granulitic xenoliths in Tertiary Hannuoba basalt, Hebei Province: Petrology and P-T estimation, paper presented at the 30th International Geological Congress, IUGS, Beijing, 1996.

Christensen, N.I., Compressional wave velocities in possible mantle rocks to pressures of 30 kilobars, *J. Geophys. Res.*, *79*, 407-412, 1974.

Christensen, N.I., Pore pressure, seismic velocity, and crustal structure, in *Geophysical Framework of the Continental United States*, edited by L.C. Pakiser and W.D. Mooney, *Mem. Geol. Soc. Am.*, *172*, 783-799, 1989.

Christensen, N.I., and W.D. Mooney, Seismic velocity structure and composition of the continental crust: A global view, *J. Geophys. Res.*, *100*, 9761-9788, 1995.

Ellis, D.J., and D.H. Green, An experimental study of the effect of Ca upon garnet-clinopyroxene Fe-Mg exchange equilibria, *Contrib. Mineral. Petrol.*, *71*, 13-22, 1979.

Fan, Q.-C., R.-X. Liu, H.-M. Li, N. Li, J.-L. Sui, and Z.-R. Ling, Rare earth element geochemistry and zircon geochronology of Hannuoba granulite xenoliths (in Chinese), *Chin. Bull. Sci.*, *43*, 133-137, 1998.

Feng, J.-L., M.-Z. Xie, H. Zhang, and W.-X. Li, The Hannuoba basalt and upper mantle xenoliths, *J. Hebei Coll. Geol.*, *1*, 45-63, 1982.

Fountain, D.M., The Ivrea-Verbano and Strona-Ceneri zones, northern Italy: A cross-section of the continental crust—New evidence from seismic velocities of rock samples, *Tectonophysics*, *33*, 145-165, 1976.

Fountain, D.M., and N.I. Christensen, Composition of the continental crust and upper mantle: A review, in *Geophysical Framework of the Continental United States*, edited by L.C. Pakiser and W.D. Mooney, *Mem. Geol. Soc. Am., 172*, 711-742, 1989.

Fountain, D.M., M.H. Salisbury, and J. Percival, Seismic structure of the continental crust based on rock velocity measurements from the Kapuskasing Uplift, *J. Geophys. Res., 95*, 1167-1186, 1990.

Gao, S., B.-R. Zhang, Z.-M. Jin, H. Kern, T.-C. Luo, and Z.-D. Zhao, How mafic is the lower continental crust?, *Earth Planet. Sci. Lett., 106*, 101-117, 1998.

Gebrande, H., Elastic wave velocities and constants of elasticity of rocks-forming minerals, in *Physical Properties of Rocks*, vol.1b, edited by G. Angenheister, pp. 1-96, Springer-Verlag, New York, 1982.

Griffin, W.L., and S.Y. O'Reilly, The composition of the lower crust and the nature of the continental Moho—Xenolith evidence, in *Mantle Xenoliths*, edited by P.H. Nixon, pp. 413-430, Elsevier Sci., New York, 1987.

Griffin, W.L., A. Zhang, S.Y. O'Reilly, and C.G. Ryan, Phanerozoic evolution of the lithosphere beneath the Sino-Korean craton, in *Mantle Dynamics and Plate Interaction in East Asia, Geodyn. Ser.*, vol. 27, edited by M.F.J. Flower et al., pp. 107-126, AGU, Washington, D.C., 1998.

Holbrook, W.S., W.D. Mooney, and N.I. Christensen, The seismic velocity structure of the deep continental crust, in *Lower Continental Crust*, edited by D.M. Fountain, R. Arculus and R. Kay, pp. 1-43, Elsevier Sci., New York, 1992.

Jackson, I., and R.J. Arculus, Laboratory wave velocity measurements on lower crustal xenoliths from Calcutteroo, South Australia, *Tectonophysics, 101*, 185-197, 1984.

Jackson, I., R.L. Rudnick, S. O'Reilly, and C. Bezant, Measured and calculated elastic wave velocities for xenoliths from the lower crust and upper mantle, *Tectonophysics, 173*, 207-210, 1990.

Kern, H., Effect of high temperature and high confining pressure on compressional wave velocities in quartz-bearing and quartz-free igneous and metamorphic rocks, *Tectonophysics, 44*, 185-203, 1978.

Kern, H., Physical properties of crustal and upper mantle rocks with regards to lithosphere dynamics and high pressure mineralogy, *Phys. Earth Planet. Inter., 79*, 113-136, 1993.

Kern, H., and A. Richter, Compressional and shear wave velocities at high temperature and confining pressure in basalts from the Faeroe islands, *Tectonophysics, 54*, 231-252, 1979.

Kern, H., and A. Richter, Temperature derivatives of compressional and shear wave velocities in crustal and mantle rocks at 6 kbar confining pressure, *J. Geophys.*, 49, 47-56, 1981.

Kern, H., and V. Schenk, Elastic wave velocities in rocks from a lower crustal section in southern Calabria (Italy), *Phys. Earth Planet. Inter., 40*, 147-160,1985.

Kern, H., and V. Schenk, A model of velocity structure beneath Calabria, south Italy, based on laboratory data, *Earth Planet. Sci. Lett., 87*, 325-337, 1988.

Kern, H., C. Walther, E.R. Fluh, and M. Marker, Seismic properties of rocks exposed in the POLAR profile region—Constraints on the interpretation of the refraction data, *Precambrian Res., 64*, 169-187, 1993.

Kern, H., L. Burlini, and I.V. Ashchepkov, Fabric-related seismic anisotropy in upper-mantle xenoliths: Evidence from measurements and calculations, *Phys. Earth Planet. Inter., 95*, 195-209, 1996a.

Kern, H., S. Gao, and Q.-S. Liu, Seismic properties and densities of middle and lower crustal rocks exposed along the North China Geoscience Transect, *Earth Planet. Sci. Lett., 139*, 439-455, 1996b.

Kern, H., B. Liu, and T. Popp, Relationship between anisotropy of *P* and *S* wave velocities and anisotropy of attenuation in serpentinite and amphibolite, *J. Geophys. Res., 102*, 3051-3065, 1997.

Kern, H., S. Gao, Z.-M. Jin, T. Popp, and S.-Y. Jin, Petrophysical studies on rocks from the Dabie Ultrahigh-Pressure (UHP) Belt, Central China: Implications for the composition and delamination of the lower crust, *Tectonophysics, 301*, 191-215, 1999.

Le Bas, M.J., and A.L. Streckeisen, The IUGS systematics of igneous rocks, *J. Geol. Soc. London, 148*, 825-833, 1991.

Liu, D.-Y., A.P. Nutman, W. Compston, J.S. Wu, and Q.-H. Shen, Remnants of >3800 Ma crust in the Chinese part of the Sino-Korean craton, *Geology, 20*, 339-342, 1992.

Liu, Y.-S., Geochemistry of lower crustal xenoliths from Hannuoba basalt: Geodynamic implications (in Chinese), Ph.D. thesis, China Univ. of Geosci., Wuhan, 1999.

Miller, D.J., and N. Christensen, Seismic signature and geochemistry of an island arc: A multidisciplinary study of the Kohistan accreted terrane, northern Pakistan, *J. Geophys. Res., 99*, 11,623-11,642, 1994.

O'Reilly, S.Y., I. Jackson, and C. Bezant, Equilibration temperature and elastic wave velocities for upper mantle rocks from eastern Australia: Implications for the interpretation of seismological models, *Tectonophysics, 185*, 67-82, 1990.

Popp, T., and H. Kern, The influence of dry and water saturated cracks on seismic velocity of crustal rocks—A comparison of experimental data with theoretical model, *Surv. Geophys., 15*, 443-465, 1994.

Powell, M., and R. Powell, A nepheline-alkali feldspar geothermometer, *Contrib. Mineral. Petrol., 62*, 193-204, 1977.

Roberts, S.J., and J. Ruiz, Geochemistry of exposed granulite facies terrains and lower crustal xenoliths in Mexico, *J. Geophy. Res., 94*, 7961-7974, 1989.

Rudnick, R.L., Xenoliths—Samples of the lower continental crust, in *Continental Lower Crust*, edited by D.M. Fountain, R. Arculus, and R.W. Kay, pp. 269-316, Elsevier Sci., New York, 1992.

Rudnick, R.L., and D.M. Fountain, Nature and composition of the continental crust: A lower crustal perspective, *Rev. Geophys., 33*, 267-309, 1995.

Rudnick, R.L., and I. Jackson, Measured and calculated elastic wave speeds in partially equilibrated mafic granulite xenoliths: Implications for the properties of an underplated lower continental crust, *J. Geophys. Res., 100*, 10,211-10,218, 1995.

Rudnick, R.L., and T. Presper, Geochemistry of intermediate- to high-pressure granulites, in *Granulites and Crustal Evolution*, edited by D. Vielzeuf and P. Vidal, pp. 523-550, Kluwer Acad., Norwell, Mass., 1990.

Salisbury, M.H., and D.M. Fountain, The seismic velocity and Poisson's ratio structure of the Kapuskasing uplift from laboratory measurements, *Can. J. Earth Sci., 31*, 1052-1063, 1994.

Sachtleben, T., and H.A. Seck, Chemical control of Al-solubility in orthopyroxene and its implications on pyroxene geothermometry, *Contrib. Mineral. Petrol., 78*, 157-165, 1981.

Wells, P.R.A., Pyroxene thermometry in simple and complex systems, *Contrib. Mineral. Petrol., 62*, 129-139, 1977.

Wood, B.J., Solubility of aluminia in orthopyroxene coexisting with garnet, *Contrib. Mineral. Petrol., 46*, 1-15, 1974.

Xu, X., S.Y. O'Reilly, W.L. Griffin, X. Zhou, and X.L. Huang, The nature of the Cenozoic lithosphere at Nushan, eastern China, in *Mantle Dynamics and Plate Interaction in East Asia, Geodyn. Ser.*, vol. 27, edited by M.F.J. Flower et al., pp. 167-195, AGU, Washington, D.C., 1998.

Zhai, M.-G., *Granulites and Lower Continental Crust in North China Archean Craton*, Seismol. Press, Beijing, 1996.

Zhu, B.-Q., *Theory and Applications of Isotope Systematics in Geosciences: Evolution of Continental Crust and Mantle in China* (in Chinese), Sci. Press, Beijing, 1998.

Zhu, Y.-P., X.-K. Zhang, and J.-S. Zhang, Crustal and upper mantle velocity structure of the Beijing-Huai'an-Fengzhen profile (in Chinese), *Seismol. Acta, 19*, 499-505, 1997.

S. Gao, Department of Geology, Northwest University, Xi'an 710069, China. (gaoshan@cug.edu.cn)

J.-L. Feng, Department of Geology, Shijiazhuang College of Economics, Shijiazhuang, China.

S.-Y Jin, Z.-M. Jin, Y.-S. Liu, Z.-B. Zhao, Faculty of Earth Sciences, China University of Geosciences, Wuhan 430074, China.

H. Kern and T. Popp, Institut für Geowissenschaften, Universität Kiel, Olshausenstrasse 40, 24098 Kiel, Germany.

M. Sun, Department of Earth Sciences, The University of Hong Kong, Pokfulam Road, Hong Kong.

(Received July 7, 1999; revised February 16, 2000;
accepted March 22, 2000.)